

RSC Advances



This is an *Accepted Manuscript*, which has been through the Royal Society of Chemistry peer review process and has been accepted for publication.

Accepted Manuscripts are published online shortly after acceptance, before technical editing, formatting and proof reading. Using this free service, authors can make their results available to the community, in citable form, before we publish the edited article. This *Accepted Manuscript* will be replaced by the edited, formatted and paginated article as soon as this is available.

You can find more information about *Accepted Manuscripts* in the [Information for Authors](#).

Please note that technical editing may introduce minor changes to the text and/or graphics, which may alter content. The journal's standard [Terms & Conditions](#) and the [Ethical guidelines](#) still apply. In no event shall the Royal Society of Chemistry be held responsible for any errors or omissions in this *Accepted Manuscript* or any consequences arising from the use of any information it contains.

Nanocrystalline Cellulose Grafted Random Copolymers of N-isopropylacrylamide and Acrylic acid Synthesized by RAFT Polymerization: Effect of Different Acrylic acid Contents on LCST Behavior

Elnaz Zeinali¹, Hossein Roghani-Mamaqani^{2}, Vahid Haddadi-Asl^{1*}*

¹Department of Polymer Engineering and Color Technology, Amirkabir University of Technology, P.O. Box 15875-4413, Tehran, Iran.

²Department of Polymer Engineering, Sahand University of Technology, P.O. Box 51335-1996, Tabriz, Iran.

ABSTRACT

Free and nanocrystalline cellulose (NCC) attached homopolymers of N-isopropylacrylamide and acrylic acid (AA) as temperature- and pH-sensitive materials and also their dual-sensitive copolymers with different contents of AA were synthesized by RAFT polymerization. NCCs were obtained from microcrystalline cellulose by an acid hydrolysis process. Then, surface of

* Corresponding authors: Tel/Fax: +98 411 3459089. E-mail addresses: r.mamaghani@sut.ac.ir (H. Roghani-Mamaqani), haddadi@aut.ac.ir (V. HAddadi-Asl)

NCC was chemically modified by 2- (dodecylthiocarbonothioylthio)-2-methylpropionic acid (DDMAT) as chain transfer agent. In situ synthesis of polymers in the presence of 1 wt% of NCC was carried out at 70 °C via R-group approach. Successful attachment of DDMAT and polymer chains on the backbone of NCC was studied by X-ray photoelectron (XPS), Fourier transform infrared, proton nuclear magnetic resonance, and Raman spectroscopies. Elemental analysis, thermogravimetric analysis, and XPS were also used to evaluate the grafting of DDMAT and polymers. Thermal behaviour of the NCC-attached polymers was also studied by differential scanning calorimetry. The lower critical solution temperatures (LCST) of polymers as phase separation temperatures were measured by the cloud point method using dynamic light scattering. Addition of NCC, AA content, and pH at higher pH values results in increase of LCST. At low pH values, increase of LCST is occurred by increase of NCC and also pH value. Morphology and crystalline structure of polymer-grafted NCCs were examined by transmission electron microscopy and X-ray diffraction respectively.

KEYWORDS: Nanocrystalline cellulose, N-isopropylacrylamide, Acrylic acid, RAFT polymerization, Lower critical solution temperature, Temperature sensitivity, and pH sensitivity.

1. INTRODUCTION

Copolymers based on poly (acrylic acid) (PAA) and poly (N-isopropylacrylamide) (PNIPAAm) attracted a great deal of interest because of their dual responsive behaviors. PAA is a pH-sensitive polymer which precipitates at $\text{pH} < 4$ in aqueous solutions for the reason of its carboxyl groups protonation. PNIPAAm shows lower critical solution temperature (LCST) in aqueous solutions because of its phase transition at about 32 °C [1, 2]. Although

thermoresponsive polymers are soluble in water at low temperatures, they separate upon heating because of the delicate balance between the hydrophobic and hydrophilic interactions [3]. This spontaneous process is endothermic and is driven by increasing entropy accompanied with the release of hydrophobically bound water molecules [4]. LCST of these temperature sensitive polymers can be tuned by copolymerization with other monomers. A more hydrophilic comonomer raises the LCST and a more hydrophobic comonomer lowers the LCST [5]. Sensitive comonomers to pH in copolymerization with N-isopropylacrylamide (NIPAAm) can increase LCST as the phase separation temperatures to 37 °C [5, 6]. Random copolymers of NIPAAm with carboxylic acid monomers of acrylic acid and methacrylic acid have been carried out using free radical polymerization techniques [6, 7]. Random copolymers of NIPAAm and AA respond to the combined external stimuli of temperature and pH. Addition of acrylic acid comonomer content results in an increase of LCST value at all pH ranges, which is mainly on account of the higher hydrophilicity of acrylic acid compared with NIPAAm. Also, because of the low value of pK_a for the acrylic acid polymers, the phase transition of the resultant copolymers are usually falls below pH 5 [6-9]. Consequently, tailoring NIPAAm copolymers which respond to the physiologically relevant pHs between 5.0 and 7.4 can be a challenge [10]. Surfing the literature reveals that composition, molecular architecture, molecular weight, and solution concentration affect the micellar properties [11-14].

Design of nanocomposites based on renewable natural resources which are biodegradable and nontoxic is very interested. Nanocrystalline cellulose (NCC) with a very high modulus of elasticity, high aspect ratio, specific surface area in the range of 150-300 m²/g, low density, easy production by acid hydrolysis of extremely abundant cellulose resources, nonabrasive nature, and recyclability have attracted considerable attention for exploring new applications in the

production of biobased nanocomposites [15-17]. Besides these, NCC is economically interested since it can be prepared from a wide variety of natural sources and used to prepare new ecologically friendly biocomposites. NCC because of its renewability, high mechanical properties and its formability into different structures can be a good support for hydrogels [18]. It is an ideal carrier for many functional polymers, like electro-conductive polymers [19]. Poly (4-vinylpyridine) coated NCC can also have reversible flocculation and sedimentation behavior with changes in pH which may offer new applications for biomedical devices, as clarifying agents, and in industrial separation processes [20]. Enzyme immobilization, drug delivery, biosensor, and many other applications can be given from the NNC composites [21-24].

Chemical nature of cellulose causes that NCC surface bears numerous hydroxyl functions which can be used for grafting reactions. Commonly, there are three methods for the covalent attachment of polymers to the surface of a substrate, which are “grafting from”, “grafting through”, and “grafting to” methods. The “grafting from” method, which has commonly been used for synthesis of graft polymer chains, relies on the surface functionalization of substrates by a polymer precursor and subsequent propagation of polymer chains from the surface-attached initiators by in situ polymerization.

Controlled radical polymerization (CRP) which results in polymers with narrow molecular weight distribution and well-defined topology has been studied numerously in the preparation of graft polymers [25, 26]. Atom transfer radical polymerization (ATRP) and reversible addition fragmentation chain transfer (RAFT) are the two common methods of CRP to prepare functional polymers. Functionality in polymers plays a key role in synthesis of graft polymer chains on various substrates. Therefore, in situ CRP has attracted a great deal of interest in synthesis of various graft polymers in the recent years [27–31].

Cellulose and its nanocrystalline parts have commonly been used for synthesis of biodegradable based nanocomposites by in situ CRP methods with grafting from approach [32–43]. Glaied et al. reported synthesis of cellulose fibers densely grafted with poly[2-(methacryloyloxy)ethyl]-trimethylammoniumchloride through aqueous ATRP [32]. They exploit the hydroxyl groups present on the cellulose surface to attach the ATRP initiator. Morandi et al. reported a similar way to synthesize polystyrene-grafted NCCs by surface initiated ATRP [33]. By a similar procedure, synthesis of temperature sensitive copolymers of poly(N,N-dimethylaminoethyl methacrylate)- and polystyrene-grafted NCCs were carried out by Yi et al. [34, 35]. Considering RAFT polymerization, Stenzel et al. were the first that report preparation of trithiocarbonate-based chain transfer agent (CTA) on cellulose and also hydroxyisopropyl cellulose to obtain polystyrene comb polymers via the Z-group approach [36, 37]. Roy et al. synthesized polystyrene-grafted cellulose [38]. They converted hydroxyl groups of the cellulose fiber into thiocarbonylthio-based CTA, and further used to mediate the RAFT polymerization of styrene. Roy et al. also polymerized 2-(Dimethylamino)ethyl methacrylate from cellulosic filter paper via RAFT polymerization [39]. Hiltunen et al., Fleet et al., and Semsarilar et al. reported similar studies using hydroxypropyl, methyl, and ethyl hydroxyethyl cellulose [40-42]. Also, Barsbay et al. grafted sodium 4-styrenesulfonate from cellulose by RAFT polymerization via 4-cyanopentanoic acid dithiobenzoate mediation [43].

Grafting of responsive polymers on substrates can also affect the characteristics of the grafted chains, their conformation in solution, and therefore their phase transition behavior. In this study, we report our investigation of the grafting NIPAAm and AA random copolymers on the surface of NCC by RAFT polymerization. According to our knowledge, there is not a comprehensive report on graft reaction of dual responsive polymers on NCC by RAFT polymerization. NCC

with its hydrophilic OH groups is used as the bio-based nanofiller which can result in increasing of LCST. Therefore, synthesis of NIPAAm and AA homopolymers and also their random copolymers by RAFT polymerization, in situ grafting of the polymers on NCC via R-approach RAFT polymerization, investigation of the effect of NCC on LCST and response of the copolymers, study the effect of various contents of AA feed content on LCST and response of the copolymers, and finally on the thermal behavior of the products are evaluated in this study.

2. EXPERIMENTAL SECTION

Materials

N-isopropylacrylamide (NIPAAm, Aldrich, 97%) was recrystallized twice from hexane and dried under vacuum prior to use. Acrylic acid (AA, Aldrich, 99%) was distilled and stored at -40 °C. Azobisisobutyronitrile (AIBN, Aldrich, 98%) was recrystallized twice from methanol. Tricaprylylmethylammonium chloride (Aldrich), 1-dodecanetriol (Riedel-de Haen, 99%), carbon disulfide (Sigma-Aldrich, >99%), sodium hydroxide (NaOH, Merck), acetone (Merck), chloroform (Merck), *n*-hexane (sigma-Aldrich, >95%), 2-propanol (Merck) were used without any purification for the synthesis of DDMAT. Microcrystalline cellulose (MCC, Aldrich), sulfuric acid (H₂SO₄, Merck), N,N'-dicyclohexylcarbodiimide (DCC, Aldrich, 99%), 4-dimethylaminopyridine (DMAP, Aldrich, 99%), methanol (Merck, 99%) were used in the preparation of functional NCC. Also, tetrahydrofuran (THF, Merck) was used as solvent in polymer separation.

Characterization

Particle size and its distribution was analyzed using a dynamic light scattering instrument (DLS, Malvern Nano Zetasizer ZS 90, United Kingdom) with a scattering angle of 176.1. The

measurement was done after the samples were diluted by diethyl ketone. X-ray photoelectron spectroscopy (XPS) was carried out on a Gammatdata-Scienta Esca 200 hemispherical analyzer equipped with an Al K α (1486.6 eV) x-ray source. Elemental analysis was carried out with an Elementar Vario max CHNOS Analyser (Hanau, German). Total carbon, hydrogen, nitrogen, and oxygen were determined by dry combustion method. Raman spectra were collected in the range from 3500 to 400 cm⁻¹ using Bruker Dispersive Raman Spectrometer fitted with a 785 nm laser source, a CCD detector, and a confocal depth resolution of 2 μ m. The laser beam was focused on the sample using an optical microscope. Fourier transform infrared (FTIR) spectra were recorded on a Bomem FTIR spectrophotometer within a range of 500–4000 cm⁻¹ using a resolution of 4 cm⁻¹. An average of 32 scans has been reported for each sample. The cell pathlength was kept constant during all the experiments. Samples were prepared on a KBr pellet in vacuum desiccators under a pressure of 0.01 torr. ¹H NMR (300 MHz) spectra were recorded on a Bruker Avance 300 spectrometer using CDCl₃ as the solvent and tetramethylsilane as the internal standard. A pulse delay of 1 s was used to ensure complete relaxation of spins. Thermal gravimetric analyses were carried out with a PL thermo-gravimetric analyzer (Polymer Laboratories, TGA 1000, UK). The thermograms were obtained from ambient temperature to 700 °C at a heating rate of 10 °C/min. A sample weight of about 10 mg was used for all the measurements, and nitrogen was used as the purging gas at a flow rate of 50 ml/min. Thermal analysis was carried out using a differential scanning calorimetry (DSC) instrument (NETZSCH DSC 200 F3, Netzsch Co, Selb/Bavaria, Germany). Nitrogen at a rate of 50 ml/min was used as the purging gas. Aluminum pans containing 2–3 mg of the samples were sealed using the DSC sample press. The samples were heated from ambient temperature to 250 °C at a heating rate of 10 °C/min. T_g was obtained as the inflection point of the heat capacity jump. X-ray diffraction

(XRD) patterns were collected on an X-ray diffraction instrument (Siemens D5000) with a Cu target ($\lambda=0.1540$ nm) at room temperature. The system consists of a rotating anode generator, and operated at 35 kV and a current of 20 mA. The samples were scanned from 2 to 40° at the step scan mode, and the diffraction pattern was recorded using a scintillation counter detector. The basal spacing of the samples was calculated using the Bragg's equation ($\lambda=2d\sin\theta$). A Vega Tescan SEM was used to evaluate the morphology of NCCs which were gold-coated using a sputtering coater. A transmission electron microscope, Philips EM 208, with an accelerating voltage of 120 kV was used to study the morphology of the NCC and NCC-grafted polymers.

Synthesis of 2-(dodecylthiocarbonothioylthio)-2-methylpropionic acid (DDMAT)

DDMAT was synthesized by a similar way to the previously reported procedure [44]. 1-dodecanethiol (20.2 g), acetone (58.0 g), and tricaprylylmethylammonium chloride (1.0 g) were cooled to 0 °C under nitrogen atmosphere and subsequently aqueous sodium hydroxide (50%) (8.4 g) was added over 10 min. After the mixture was stirred for an additional 20 min, carbon disulfide (7.6 g) in acetone (10.0 g) was added over 30 min. After addition of chloroform (17.8 g), aqueous sodium hydroxide (50%, 40 g) was added dropwise and stirring was continued overnight. 200 ml of water and 80 ml of concentrated HCL were added to acidify the aqueous solution. After removing acetone, the solid was collected, and then stirred in 300 ml of 2-propanol. The resulting solid was recrystallized from hexane to afford 22.0 g of yellow crystalline solid (mp \approx 60 °C).

^1H NMR (in CDCl_3): δ 1.0 (t, 3H), 1.30-1.5 (m, 18H), 1.6-1.8 (m, 8H), 3.2 (t, 2H), 11.0 (s, 1H).

FTIR: 2849 cm^{-1} (CH), 1716 cm^{-1} (C=O), 1069 cm^{-1} (C=S), 814 cm^{-1} (C-S).

Preparation of NCC from the source of MCC

NCC was prepared by acid hydrolysis of MCC similar to the literature [45, 46]. MCC powder (10.0 g) was hydrolyzed by sulphuric acid (87.5 ml, 64% w/v) for 5 h at 45 °C. The hydrolysis was quenched by adding a large amount of water (500 ml). The resulting mixture was cooled to room temperature and centrifuged. Water (500 ml) was added to the precipitate and the mixture was then sonicated. Then, 1.0% NaOH solution was added into the mixture and stirring was applied for 48 h. After addition of 500 ml water, centrifugation and sonication process was continued for three times. Then, the suspension was filtered using an Amicon Stirred Cell until the pH of suspension reached a constant value.

Synthesis of DDMAT-grafted NCC

NCC was modified with DDMAT similar to the literature [42]. A 50 ml round-bottom flask was charged with NCC (0.1 g) dissolved in chloroform (10 ml), DDMAT (1.0 g, 4.2 mmol), DCC (0.4 g, 1.94 mmol) of, and DMAP (0.26 g, 2.13 mmol). The reaction was sealed and placed in a preheated oil bath at 40 °C. The reaction was left to run for 6 days. The reaction mixture was then precipitated in methanol, dissolved in chloroform, and precipitated in methanol again. This cycle was repeated three times to obtain a pure product of NCC-g-CTA.

Synthesis of Polymers and Nanocomposites

Batch polymerizations were performed in glass vials which were placed in an oil bath thermostated at 70 °C. At first, monomer (14.38 g), DDMAT (0.68 g), AIBN (0.022 g), and dioxane (35.1 ml) was added into a 250-ml lab reactor and mixed for 2 h. Then, the reactor's contents were transferred into the glass vials by means of a syringe and was then degassed under the nitrogen atmosphere, sealed and placed in an oil bath. Polymerizations were run during 4 h for AA and 25 h for NIPAAm monomers. The polymerizations were stopped by cooling the reaction mixture in an ice bath after distinct time periods. Also, cool methanol was added into the

vials for precipitating polymer. Synthesis of random copolymers was accomplished similarly. However, NIPAAm (11.825 g), AA, AIBN (0.015 g), DDMAT (0.165 g) and 12.5 ml dioxane was used and polymerizations were run during 17 h. Various molar fraction of AA was 5, 10, 15, 20, and 30 molar percent. Samples are designated as the general name of PNIPAAm-co-PAAX, in which X denotes the AA molar ratio in the feed. In the case of NCC-grafted polymers, the same procedure was run other than DDMAT was added half of the amount used for polymers. Also, NCC-g-CTA (1 wt% relative to monomer) was added at the first stage of reactant addition. Samples are designated as the general name of NCC-g-PNIPAAm-co-PAAX, in which X denotes the AA molar ratio in the feed.

Separation of polymer chains from particles

The prepared nanocomposites were dissolved in THF and the polymer chains were separated from NCC by high-speed ultracentrifugation (10000 rpm). The solution was passed through a 0.2 micrometer PTFE filter and then poured into Methanol (500 mL) to precipitate polymer chains. After filtration, polymer was dried overnight in a vacuum oven at temperature 50 °C. The remained solid on the filter was the NCC-grafted Polymers. Grafted polymers were also separated from NCCs by acid hydrolysis. By a typical procedure, 0.2 g of NCC-grafted polymers with 15 mL of HCl solution and 30 mL of THF were added into a flask and stirred at 85 °C for 5 days. After that the reaction mixture was filtered and the filtrate was dried at 65 °C in a vacuum oven to give separated graft polymers.

3. RESULTS AND DISCUSSION

NCC was prepared by acid hydrolysis of MCC. During this process, small crystalline blocks of cellulose are separated from the amorphous parts. These nanocrystals are in the form of rods with an average length of below 100 nm. Figure 1 shows the SEM and TEM images for the

MCC and NCC. Cellulose microcrystals with dimension of 10-50 μm in length and 10-25 μm in diameter are clearly shown in the Figure 1 (A). These MCC granules with large sizes are composed of microfibrils with strong hydrogen bonding and nanocrystals can be obtained after acid hydrolysis [47]. Rod like shapes of NCC are also displayed in SEM and TEM images (Figure 1 (B) and (C)). NCC with length of 100-200 nm and diameter of 10-20 nm are an order of magnitude smaller than the microcrystals. Because of the nature of NCCs, they formed laterally aggregated morphology. High specific area and strong hydrogen bonds in addition to the surface ionic charge caused by acid treatment can also result in this arrangement [48]. Similar size ranges were also reported by Bai et al. for the NCCs prepared from MCC source [45]. TEM image also shows the separated nanocrystals which were obtained by dispersion of NCCs in water (0.1 wt%). DLS from 0.1 wt% solution of nanocrystals in water was used to evaluate the size of nanocrystals and its distribution and the corresponding result is displayed in Figure 1 (D). A narrow monomodal peak at the vicinity of about 107 nm clearly shows that NCCs are not accumulated and uniformly distributed in the water. Calculation of hydrodynamic radius of the nanoparticles by their diffusion coefficient in a medium from the Stokes-Einstein equation in DLS shows that the value is given by this technique is the radius of a sphere having the same diffusion coefficient as the rodlike NCCs. The size of 107 nm is close to the mean length of 130 nm reported by Azzam et al. [49] and Elazzouzi-Hafraoui et al. [50] for NCCs prepared from the source of cotton.

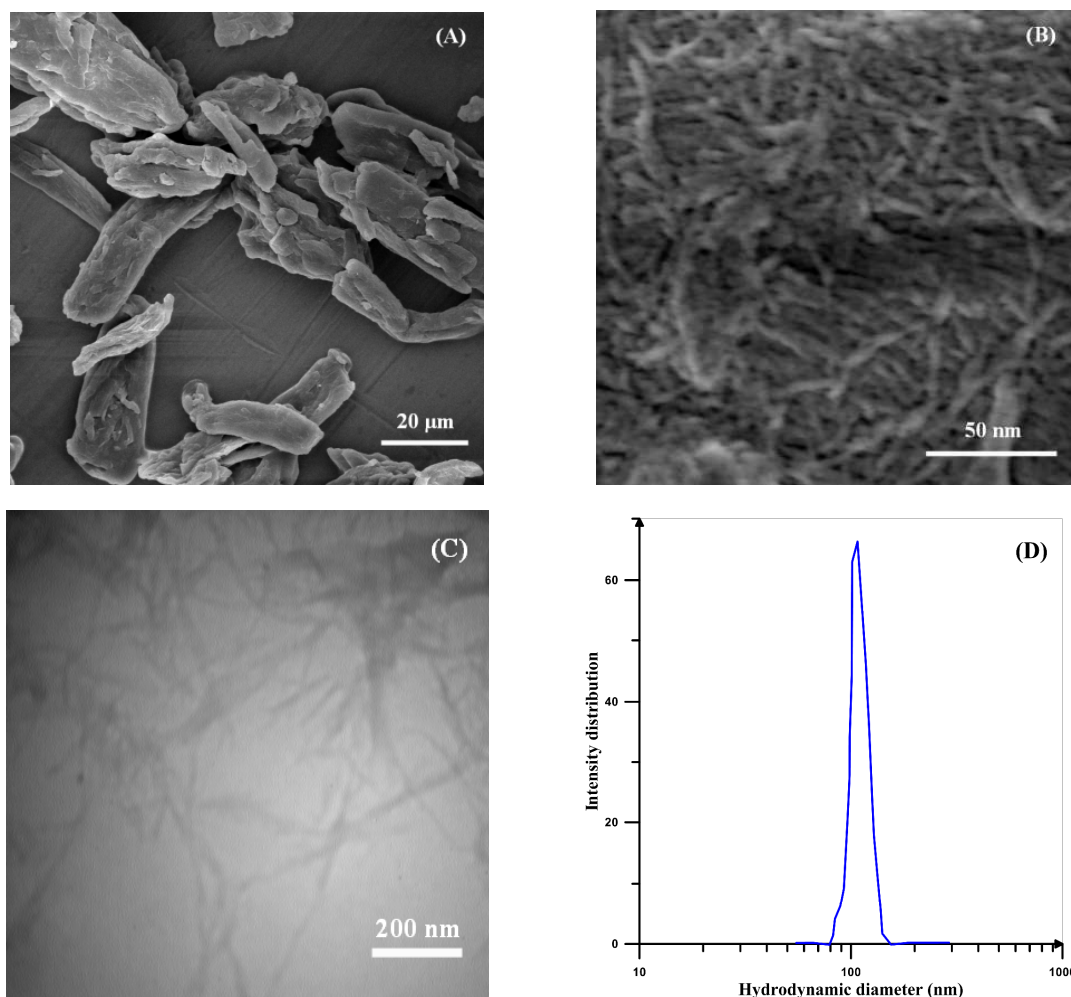


Figure 2- SEM images of (A) MCC and (B) NCC, (C) TEM image of NCC, and (D) Intensity distribution of the NCCs in water measured by DLS

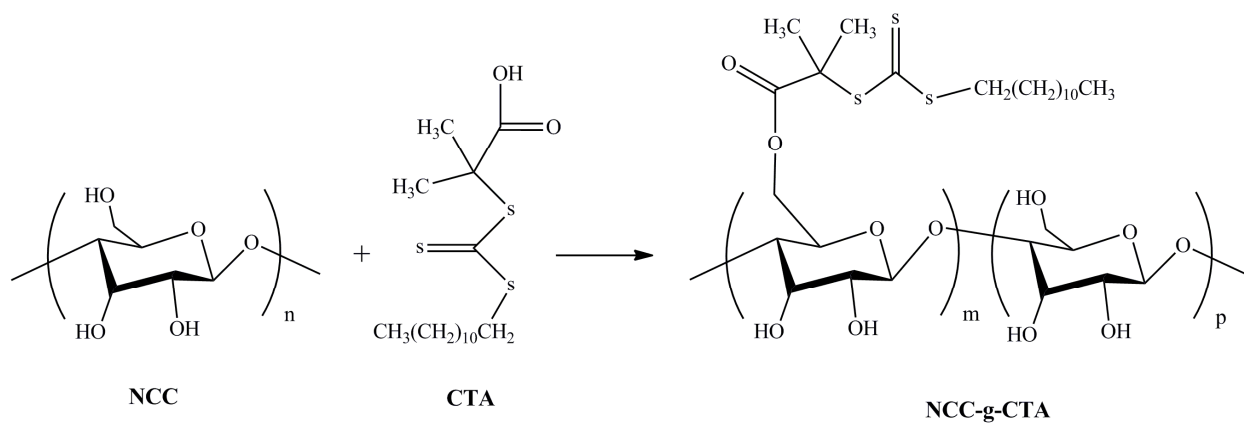


Figure 2- Synthesis of NCC-g-CTA

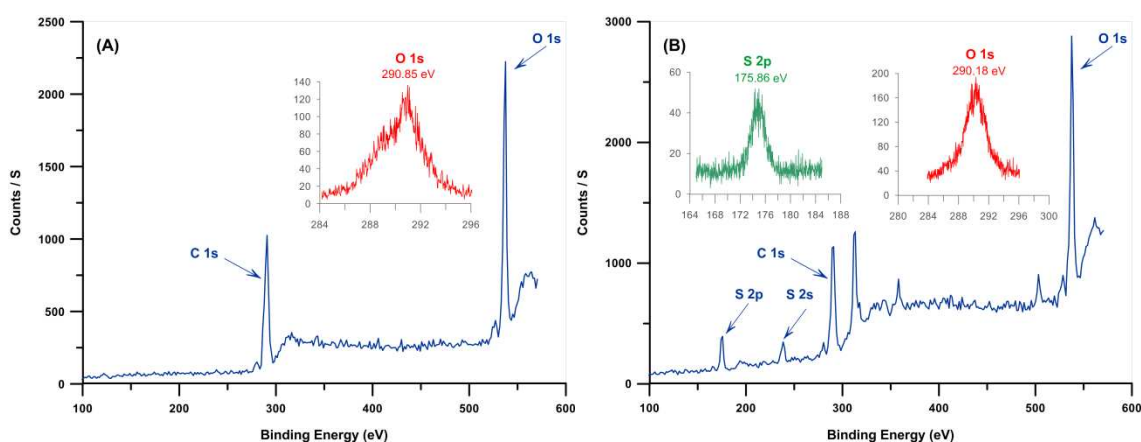
DDMAT was grafted on NCC from its R group by an esterification reaction. This insures that grafting polymers on NCC will proceed by R-approach (Figure 3). Elemental analysis and XPS were employed to investigate the grafting percent of DDMAT on NCC. Table 1 shows the content of carbon, oxygen, nitrogen, and sulfur atoms for MCC, NCC, and NCC-g-CTA. Composition of oxygen in NCC can be used for calculation of hydroxyl groups composition. Repeating units of NCC is composed of two glucose groups with the formula of $C_6H_{10}O_5$. Therefore, the amount of oxygen atoms in the form of hydroxyl group is equal to 6 in every repeating unit. Therefore, 47.9 % of oxygen in NCC shows that 28.7% of NCC consists of hydroxyl groups. According to the results of elemental analysis, total amount of sulphur atom which originates from the attached CTA is about 2.3 percents which gives C/S value of 17.74.

Table 1- Carbon, oxygen, nitrogen, and sulfur content for MCC, NCC, and NCC-g-CTA from elemental analysis

Sample	N	C	H	O	S	C/O	C/S
MCC	<0.1	45.3	6.1	47.2	<0.1	0.96	---
NCC	<0.1	44.4	5.9	47.9	<0.1	0.93	---
NCC-g-CTA	<0.1	40.8	4.9	42.1	2.3	0.97	17.74

XPS was used to investigate the surface composition of NCC and NCC-g-CTA (Figure 3 and Table 2). Figure 3 shows the survey data and also the higher resolution data of the S 2p, O 1s, and C1s areas. Survey-scan spectra of both the neat and modified NCCs show that carbon and oxygen are their main components. Survey-scan spectrum of NCC varies from the NCC-g-CTA considerably at the binding energy of 175.9 eV, which relates to sulfur. Appearance of S 2p and S 2s band spectra at the binding energies of 175.86 and 238 eV clearly shows that DDMAT has been anchored on the surface of NCC [43]. The inset of Figure 3 (B) shows the band of S 2p at 175.9 eV assigned to C–S groups. C 1s band spectrum at the binding energy of 286–294 eV is

used to evaluate the proportion of various functional groups in NCC and NCC-g-CTA, which reflects the local environments of the carbon atoms (C–C and C–H, C–O and C–S, O–C–O, O–C=O). The relative amounts of each carbon bond were determined before and after surface modification. The deconvoluted peak related to C–S bond which is observed at the binding energy of 290 eV implies the successful attachment of DDMAT on the NCC surface [51]. The results of Figure 3 (C) and (D) are presented in Table 2 and show that appearance of sulfur results in increased values of C–O/C–S and O–C=O peak area. In addition, appearance of O–C=O peak in the spectrum of NCCs shows the presence of residual cell wall polysaccharides with carboxylic groups that remain intimately linked to MCC. It may also results from the oxidation of the reducing end groups of MCC [51, 52]. The ratio of O–C–O/C–O is 0.28 which is very close to the theoretical value of 0.2 calculated from the formula of pure cellulose (C₆H₉O₅)_n. This ratio decreases to 0.23 because of the appearance of the C–S group. Sulfur content of 6.39% according to the data obtained from survey scan spectra of NCC-g-CTA shows that the graft percent of DDMAT on NCC is about 17.14% which is close the value resulted from elemental analysis.



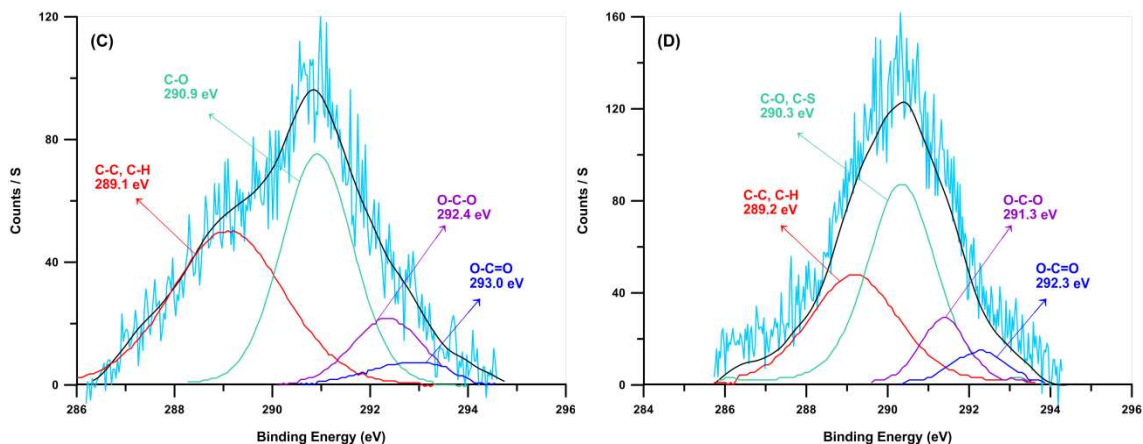


Figure 3- Wide scan XPS for (A) NCC and (B) NCC-g-CTA, and C1s core-level spectrum for the (C) NCC and (D) NCC-g-CTA

Table 2- Elemental surface composition of NCC and NCC-g-CTA resulted from XPS and surface functional group compositions obtained from the decomposition of the C1s signal

Sample	Composition (%)				Composition of C in groups			
	C	O	S	C/O	(C-C/C-H)	(C-O/C-S)	(O-C-O)	(O-C=O)
NCC	34.9	65.09	-	53.6	42.44	41.07	11.54	4.94
NCC-g-CTA	31.48	62.13	6.39	50.6	33.82	48.47	11.23	6.48

Raman spectra for NCC and NCC-g-CTA are displayed in Figure 4. Results shows that C–S and C=S peaks appear at the wave numbers of 804 and 1249 cm^{-1} respectively in the spectrum of NCC-g-CTA, which relates to DDMAT and confirms its successful attachment on NCC [38]. The peak assigned to the CH_2 and CH_3 groups of DDMAT is also observed at the wave number of 1444 cm^{-1} . In addition, C=O and O–H groups are observed at the wave numbers of 1624 and 2894 cm^{-1} respectively [43].

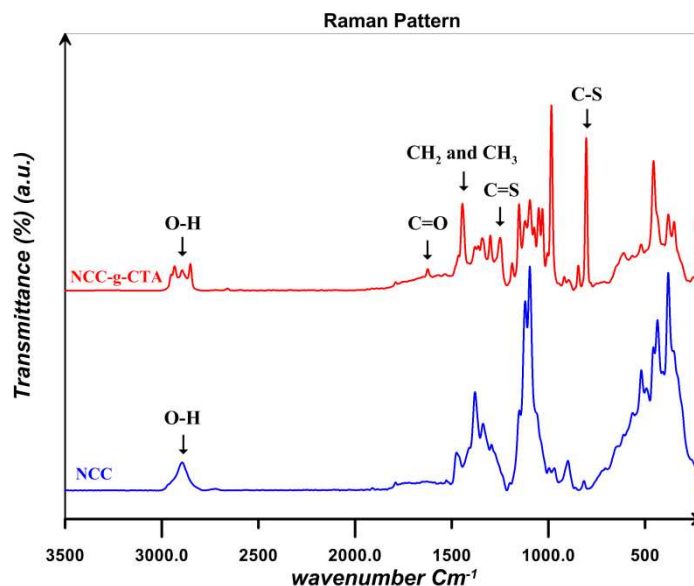


Figure 4- Raman spectra for (A) NCC and (B) NCC-g-CTA

FTIR is used to confirm the successful surface modification of NCC by DDMAT and polymers. In addition, effect of the addition of NCC on the spectra of PNIPAAm, PAA, and their random copolymers with various AA contents is studied. FTIR spectra for PNIPAAm, PAA, and their random copolymers are shown in Figure 5 (A). In the spectrum of PNIPAAm, the bands at 1538 and 1641 cm^{-1} is related to the amide groups (type I and II) [53, 54]. In addition, the peaks at 1362 and 1380 cm^{-1} are attributed to the isopropyl groups. The peaks at 1450 and 2850-2980 cm^{-1} are assigned to CH and CH_2 units. Also, stretching vibration of N-H group is seen at 3293 cm^{-1} . PAA spectra show two peaks at 1730 and 3419 cm^{-1} which are assigned to the stretching vibration of C=O and O-H groups respectively [8]. FTIR spectra confirm the formation of copolymers by the appearance of the characterization bands of PAA and PNIPAAm. By increasing AA content, C=O band area increases in the random copolymers spectra. In addition, electropositive N-H group of NIPAAm causes a shift of carbonyl wave number to lower values.

FTIR spectra for NCC, NCC-g-CTA, and polymer grafted NCCs are presented in Figure 5 (B). Bending and stretching vibrations of C–H in NCC are appeared at 1370 and 2893 cm^{-1} respectively. Water absorption of NCC causes a peak at 897 cm^{-1} which assigned to the O–H stretching vibration. The characteristic peaks at 1410 and 1640 cm^{-1} relate to the symmetric and asymmetric stretching carboxyl groups [55]. The OH stretch for NCC and NCC-g-CTA does not show a remarkable difference. This shows that DDMAT is attached to hydroxyl groups at the surface (with low percentage) and interior hydroxyl groups of the crystallite (with high percentage) remained unreacted [56]. The peak at 1635 cm^{-1} arises from the carbonyl groups of DDMAT and is a proven for successful surface modification of NCC with DDMAT. Appearance of the characteristic bands of PNIPAAm and AA in the spectra of the modified NCCs shows that grafting reactions have appropriate been carried out. The increased strength of C–H stretching vibrations at 2850-2980 cm^{-1} indicates higher amount of methylene groups in the polymer modified NCCs than in the neat NCC an NCC-g-CTA. This demonstrates the presence of polymer chains in the samples after the extraction of free chains and this is an evidence for the successful grafting reactions [52]. Polymer grafting on the surface of nanocellulose results in a decreased value of hydroxyl vibration peak area which arises from the hydrogen bonding at 3030-3680 cm^{-1} . This shows that the content of hydroxyl groups decreases during the grafting process [57].

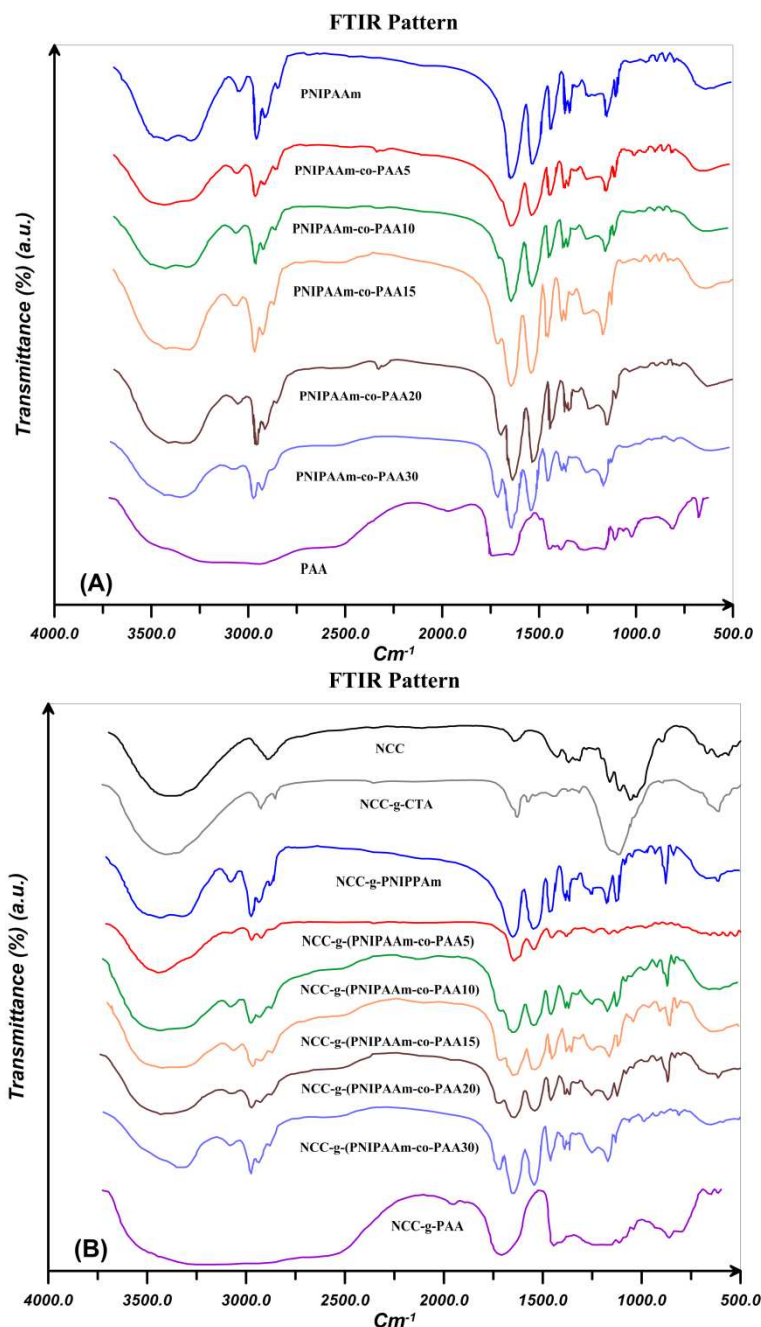


Figure 5- FTIR spectra for PNIPAAm, PAA, and their random copolymers by varying AA content (A) without and (B) in the presence of 0.1 wt% NCC

^1H NMR spectra of PNIPAAm, PAA, and their random copolymers by varying AA content are exhibited in Figure 6. Feature signals of NIPAAm ($\text{CH}-\text{CH}_3$: $\delta=1$, $\text{CH}-\text{CH}_3$: $\delta=3.7$, $\text{CH}-\text{CH}_2$: $\delta=1.4$, $\text{CH}-\text{CH}_2$: $\delta=1.8$) and DDMAT ($\text{S}-\text{CH}_2$: $\delta=3.2$, $\text{CH}_2-(\text{CH}_2)_{10}$: $\delta=1.2$) in addition to PAA

($\text{CH}_2\text{-CH}$: $\delta=1.49\text{-}1.79$, $\text{CH}_2\text{-CH}$: $\delta=2.26$) and DDMAT ($(\text{CH}_2)_{10}\text{-CH}_3$: $\delta=1$, $\text{CH}_2\text{-(CH}_2)_{10}$: $\delta=1.12$, S-CH_2 : $\delta=3.56$) can be observed in the spectra. The peak at $\delta=4.68$ is related to the solvent [8, 38]. In random copolymers, the signal at $\delta=1.2\text{-}1.6$ which arises from the hydrogen atoms ($\text{CH}_2\text{-CH}$ in NIPAAm and $\text{CH}_2\text{-CH}$ in PAA) increases with addition of AA content.

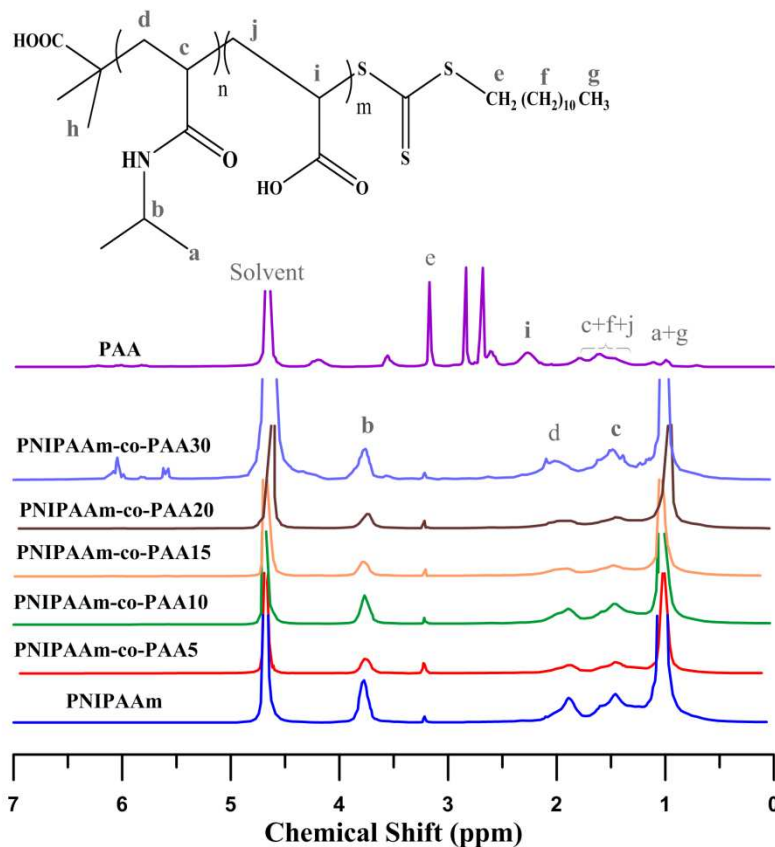


Figure 6- ^1H NMR spectra for PNIPAAm, PAA, and their random copolymers by varying AA content in D_2O

Molecular weights of the synthesized polymers calculated from ^1H NMR data are presented in Table 3. The theoretical ratio of AA in the random copolymers (F_{AA}) is necessary for the molecular weight estimation which can be obtained from the equation 1 (Mayo and Lewis) [58]:

$$F_{AA} = \frac{r_{AA}f_{AA} + f_{AA}f_{NIPAAm}}{r_{AA}f_{AA}^2 + 2f_{AA}f_{NIPAAm} + r_{NIPAAm}f_{NIPAAm}^2} \quad (1)$$

where, f_{AA} and f_{NIPAAm} are the feed ratio of AA and NIPAAm. Also, r_{AA} and r_{NIPAAm} are reactivity ratios of AA and NIPAAm respectively. In addition, theoretical number average molecular weights ($M_{n, th}$) of the polymers can be calculated from the equation 2 [1]:

$$\overline{M}_{n, th} = MW_{RAFT} + \frac{[M]_0 MW_{Monomer} \cdot P}{[RAFT]_0 + 2[AIBN]} \quad (2)$$

where, MW_{RAFT} , $MW_{monomer}$, $[M]_0$, $[RAFT]_0$, $[AIBN]_0$, and P denote the molecular weights of DDMAT and monomer, and initial concentration of monomer, DDMAT, and AIBN respectively which gives the theoretical molecular weight of 7106 gmol^{-1} for the homopolymers at $P=1$. Also, the molar ratio of AA in the copolymers can be obtained by the equation 3:

$$AA \% = \frac{A_i}{A_i + A_b} \quad (3)$$

where, A_i and A_b are peak area for the bands at $\delta=2.26$ and 3.7 remarked as i and b in Figure 6. According to the results of Table 3, AA content is higher than the feed ratio for all the copolymers. Also, AA content in the NCC-grafted copolymers is higher than the free copolymers. This may result from the polarizing effect of NCC which activates AA in the copolymerization reaction. Lower DDMAT content in the nanocomposites reaction medium results in higher molecular weights of NCC-grafted polymers. In addition, by the addition of AA content, molecular weight of the copolymers reduces which is mainly on account of the lower molecular weight of AA and also its higher propagation rate. It is also observed that molecular weight of grafted polymers is a bit higher than the free chains.

Table 3- AA content and molecular weights of the free polymers calculated from ^1H NMR

Polymer	AA%				M_n (g.mol $^{-1}$)	
	Feed	Polymer (Eq. 1)	Polymer (^1H NMR)			
			Free	NCC-grafted	Free	NCC-grafted
PNIPAAm	0	0	0	0	7455	7834
PNIPAAm-co-pAA5	5	8.5	7.3	8.1	14763	15140
PNIPAAm-co-pAA10	10	12.6	13.2	13.3	13691	14229
PNIPAAm-co-pAA15	15	18.4	16.8	18.1	11323	11892
PNIPAAm-co-pAA20	20	26.2	24.3	27.4	9212	10058
PNIPAAm-co-pAA30	30	35.6	33.8	38.3	7205	7932
PAA	100	100	100	100	5882	6302

LCST behavior for PNIPAAm and its random copolymers in solution was studied by their cloud point variations. Contribution of PAA as pH-sensitive and PNIPAAm as temperature responsive polymers results in copolymers with dual sensitive characteristics. Therefore, DLS results in two pH ranges of 3-4 and 7-8 were used to study the cloud point and LCST behavior. LCST of thermoresponsive polymers is mainly attributed to a change in the hydrophilic and hydrophobic balance of the polymers which originates from the interactions between polymer chains and water molecules and most importantly hydrogen bonding. At low temperatures, strong interactions between the polar groups and water molecules results in an appropriate solubility of the polymers. Lower entropy of water molecules surrounding apolar groups compared with the free molecules results in an entropic penalty. Increasing apolar surface area of polymer results in an increase of entropic penalty and also decrease of LCST [1].

Hydrodynamic diameter for the 0.2 wt% solutions of PNIPAAm and NCC-g-PNIPAAm at different temperatures in addition to their DLS diagrams near the LCST points are shown in Figure 7. Spatial conformation and solubility of PNIPAAm vary with temperature. At temperatures lower than LCST, strong hydrogen bonding between the polymer chains and water

molecules results in the polymer solubility. However, polymer chains collapse at temperatures higher than LCST because of hydrogen bonding between N-H and C=O [59]. PNIPAAm chains become poorly soluble and collapsed together when temperature is increased, and there is a sharp transition at 34 °C, which corresponds to the phase transition temperature of PNIPAAm. By increasing temperature, also particle size of NCC-g-PNIPAAm varies suddenly at 34 and 40 °C, which is on account of the insolubility of free and graft PNIPAAm chains at higher temperatures. PNIPAAm particle size increases from 12 to 230 nm; however, this variation occurs in two steps for nanocomposites. The first step at temperature range of 33-35 °C originates from the PNIPAAm particles which expand from 76.9 to 106 nm in diameter. The second step relates to the variation of NCC-g-PNIPAAm particle size from 116 to 222 nm. NCC particles increase water solubility of PNIPAAm because of a large number of hydroxyl groups. Therefore, an increase of about 6 °C is observed for LCST by the addition of NCC. Also, PDI values of the particles increases in the presence of NCC.

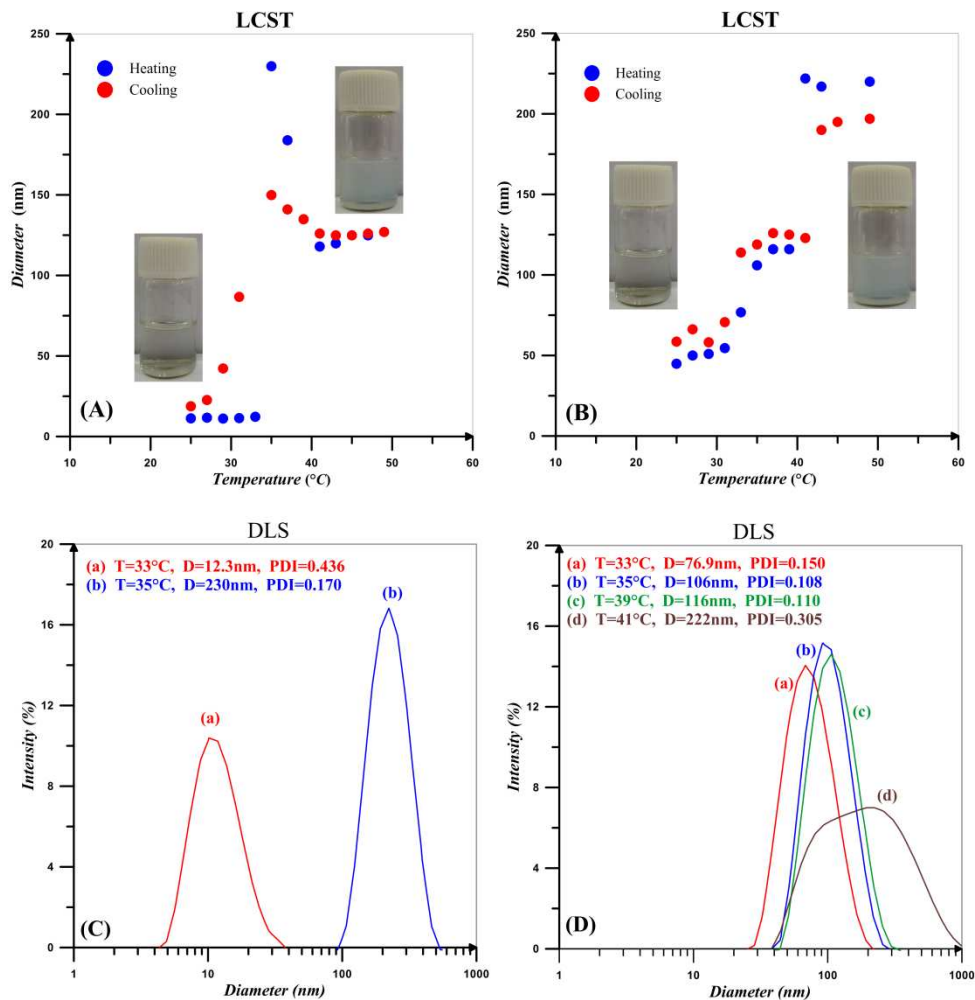


Figure 7- Hydrodynamic diameter for the 0.2 wt% solutions of (A) PNIPAAm and (B) NCC-g-PNIPAAm in addition to the DLS intensity diameters near the LCST points for (C) PNIPAAm and (D) NCC-g-PNIPAAm

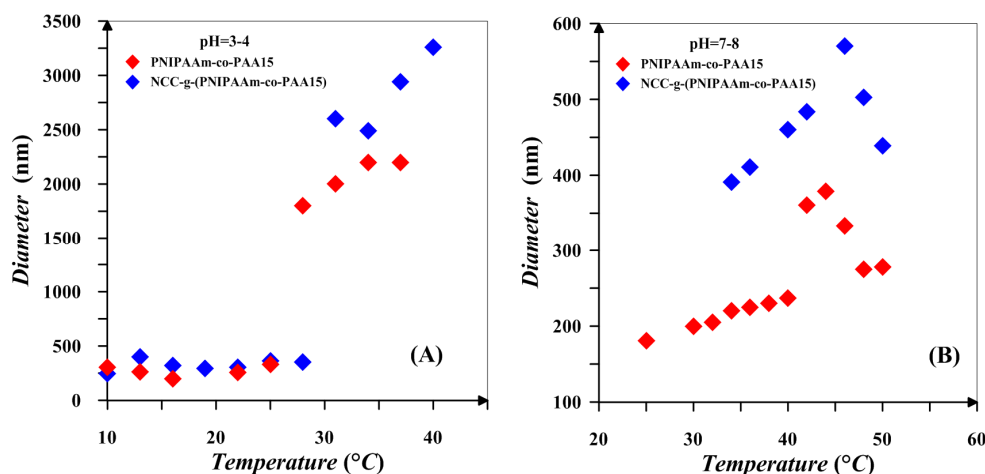


Figure 8- Effect of pH on the LCST behaviour of PNIPAAm-co-PAA15: (A) pH=3-4 and (B) pH=7-8

Effect of pH on the LCST behaviour of free and NCC-attached PNIPAAm-co-PAA15 is studied in two pH ranges of 3-4 and 7-8 and the results are shown in Figure 8. Also, LCST diagram of the 0.2 wt% solutions of NIPAAm and AA random copolymers with various AA content and also NCC-grafted copolymers in different pH values is displayed in Figure 9. Addition of AA in random copolymers results in increase of LCST point at pH=7-8; however, a decrease in LCST is observed with increasing AA content at pH=3-4. Hydrophobic behavior of AA in protic media is the main reason for decrease of LCST. In addition, hydrogen bonding between carboxylic group of AA and amide functional group of NIPAAm in protic media is reasonable. This effect was seen in random copolymers of AA and NIPAAm and also their graft copolymers [1, 60]. More ionization of the copolymers at higher pH values results in higher LCST values. Also, copolymer chains expand because of electrostatic repulsion, and therefore interaction between polymer chains decreases at higher pH values [1]. According to the inset of Figure 8, it is clear that phase transition of copolymer chains is not sharp at higher pH values. Since more of the AA units of the copolymer chains are ionized at higher pH values, their hydrophilic tendencies

interfere with the LCST behavior of the PNIPAAm segments. Therefore, aggregation of PNIPAAm chain segments to form collapsed particles is weakened. In addition, particles with lower diameters were obtained at higher pH values after phase separation. Collapse of polymer chains into large aggregates is decreased because of the stabilization of the smaller particles in the solution by ionized PAA segments. The plateau at higher pH values for the LCST variation by AA content is also reasonable because of the ionization of AA which prevents from the formation of large aggregates. Finally, by increasing pH values, ionized PAA segments reduce the effect of hydrophobically bound water and it may reach to a point that PNIPAAm segments are unable to form aggregates [1]. At both pH ranges, NCC-grafted polymers show larger diameters upon the aggregation which is mainly on account of the presence of NCC particles with the average diameter of 107 nm. Steric confinement of the NCC attached polymers results in their sharp phase transition upon heating.

It is clear that LCST can be tuned by three factors of NCC addition, AA content, and pH. Addition of NCC, AA content and pH at higher pH values results in increase of LCST. At low pH values, increase of LCST is occurred by increase of NCC and also pH value. Therefore, LCST can be tuned to desired values at a particular pH by changing the PAA content and also NCC of the copolymer. This shows that grafting density of copolymers and polymerization conversion is also key factors in tailoring the LCST. This dual sensitive NIPAAm-co-PAA copolymers and its biocomposites is tailored to switch from a hydrophobe to an ionized state at predetermined pH values. In addition, its PNIPAAm segments can switch from a soluble to collapsed parts at predetermined temperatures. Also, NCC addition hinders this behavior thermally. This dual behavior of products is useful in a variety of biomedical applications. In drug delivery, the combined sensitivity could be used to enhance drug delivery where pH

gradients are shown in body. In addition, in a desired location releasing of drugs temperature in combination of pH may act as a good controlling key.

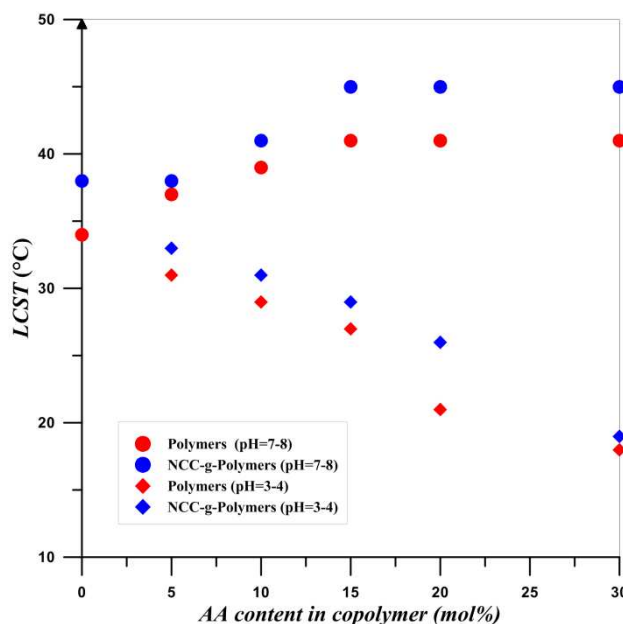
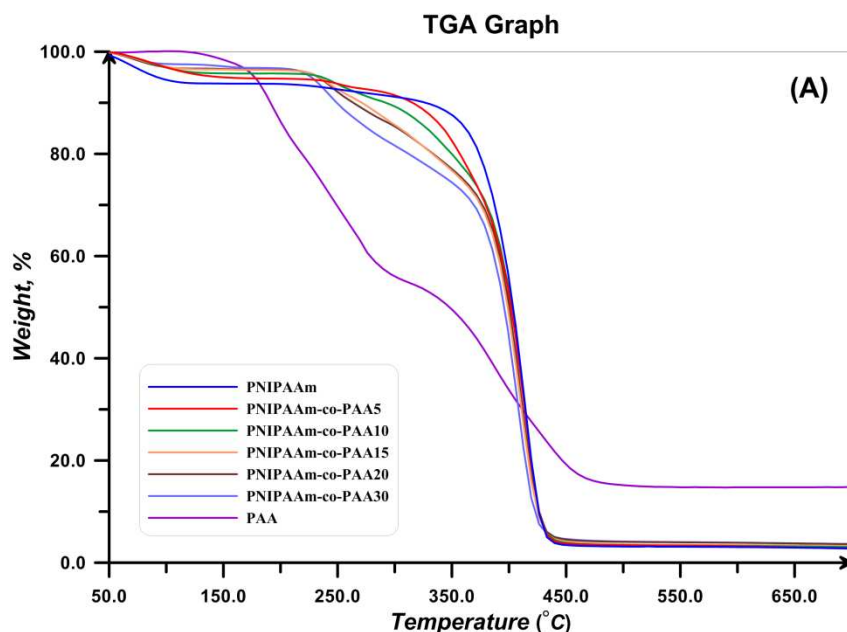


Figure 9- LCST diagram for the 0.2 wt% solutions of NIPAAm and AA random copolymers with various AA content in different values of pH

TGA and DTG thermograms for PNIPAAm, PAA, and also NIPAAm and AA random copolymers are presented in Figure 10. All the samples show a weight loss at temperatures lower than 120 °C which is attributed to the water evaporation. Degradation of PAA is carried out in three steps of hydrogen abstraction, carboxyl abstraction, and PAA chains degradation. The first step takes place by intra- and intermolecular reactions of carboxyl groups. Intramolecular reactions result in hexagonal anhydride rings (Figure 11, A). At the second step which is accomplished at temperatures higher than 200 °C, CO₂ released upon the degradation of anhydride groups (Figure 11, B). At temperatures higher than 300 °C, carboxyl abstraction process is continued. PAA repeating units remains between anhydride rings at the backbone during these processes. Broken short chains which consist of two or more repeating units are

formed during the third step at temperatures higher than 350 °C (Figure 11, C). Also, CO is released at higher temperatures [61]. Degradation temperature of random copolymers decreases with increasing AA content which results from the lower degradation temperature of PAA. In addition, their degradation process consists of some distinguished stages because of multi-stage degradation pattern of PAA. Short chains of PAA after degradation results in high values of char content for random copolymers.



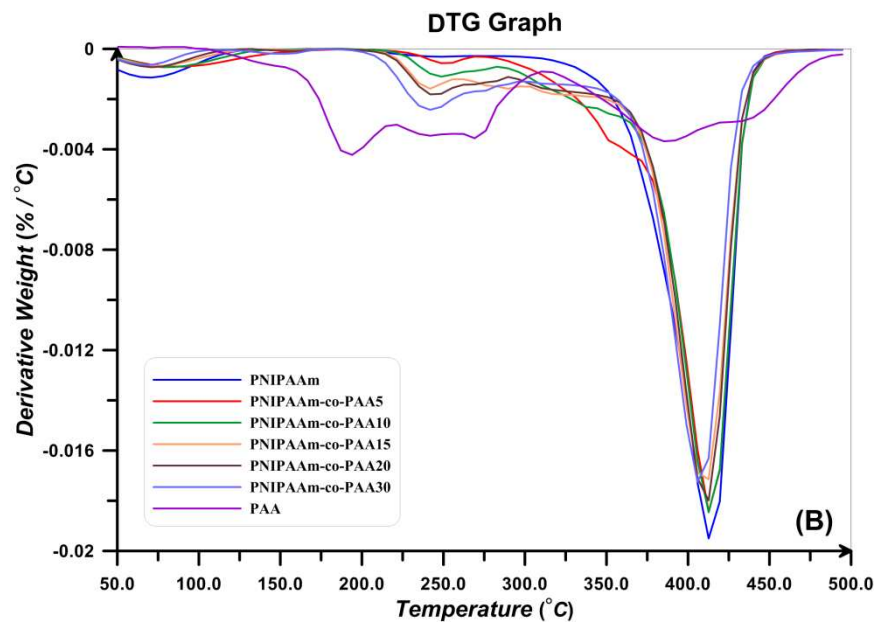


Figure 10- (A) TGA and (B) DTG thermograms for PNIPAAm, PAA, NIPAAm and AA random copolymers

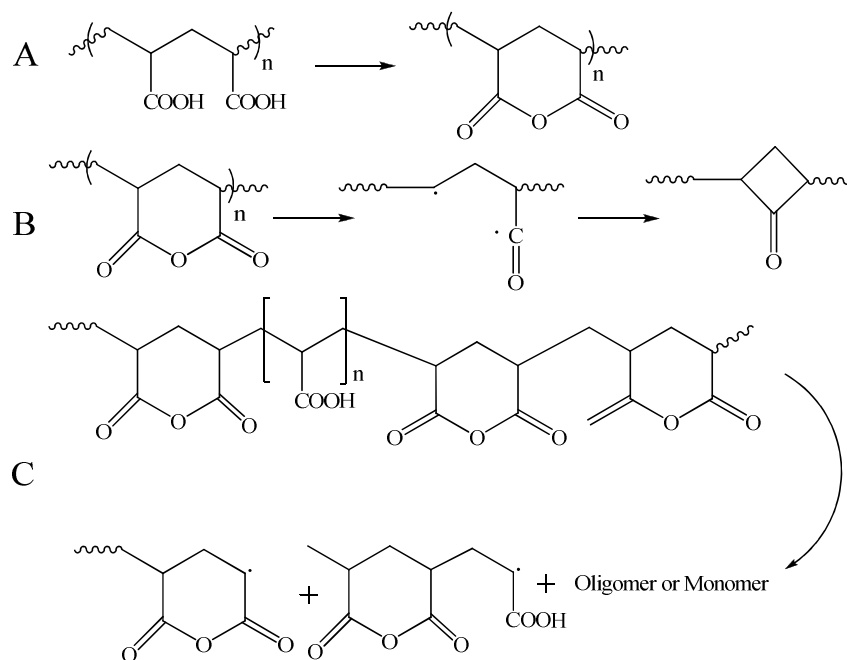
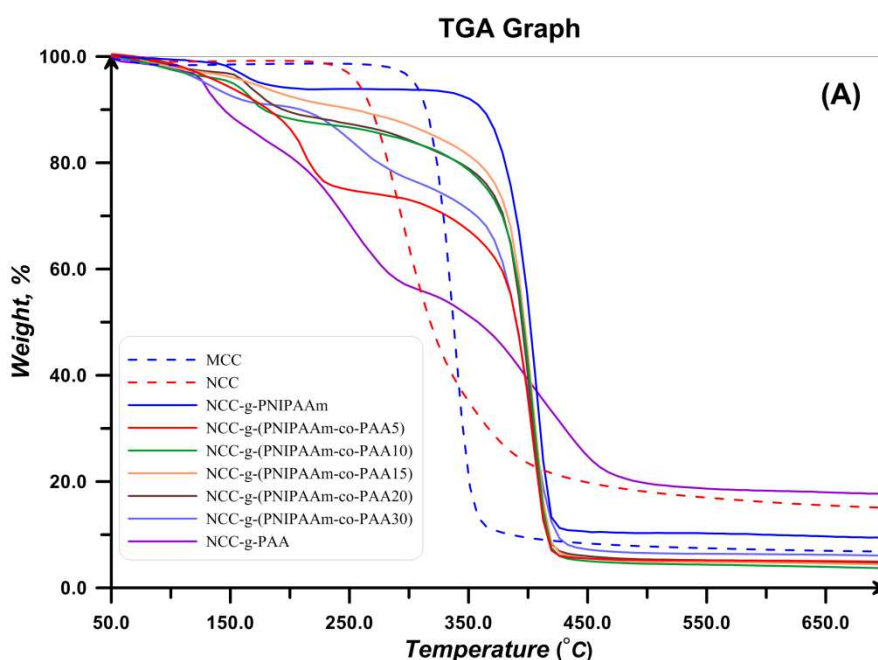


Figure 11- Degradation procedure for PAA

TGA and DTG thermograms for MCC, NCC, and polymer grafted NCCs are also shown in Figure 12. Thermal degradation behavior of NCC differs from MCC at temperatures higher than 150 °C, the decomposition of CNC started at lower temperatures (230 with respect to the 290 °C), continues in higher temperature range, and also its char value is higher. This distinction is a result of the difference in their particle size. CNC because of its small particle size and high specific surface area has higher number of free end chains in the surface which decompose at lower temperatures. The decomposition of cellulose at low temperature usually facilitated the formation of char residue (18.03 with respect to the 7.79% at 500 °C). Amorphous chains on the surface of NCC degrade at lower temperatures and results in lower thermal stability of NCC [55]. Considering DTG thermogram of NCC, its degradation takes place at one step and there is not any degradation step at temperatures in the range of 150-200 °C. It is reported that sulfate-containing NCCs show a distinguished degradation step at this region because of the presence of sulfate groups [55]. Therefore, repeated centrifugation and ultrasonic processes in combination with base treatment with NaOH results in sulfate free NCC product. Additionally, DTG peak point which is commonly known as the degradation temperature is lower for NCC (291 °C with respect to 337 °C). Moreover, deconvolution of DTG curves of NCC results in two peaks, the first one originates from the degradation of cellulose macromolecule (66.8%) and the second one is assigned to the degradation of the remained solid (33.2%).

As shown in Figure 12, the polymer-grafted NCCs displays a two-stage decomposition profile. The first degradation step is observed in temperature range of 150-220 °C. The second degradation step starts at around 410 °C, which is slightly higher than the pure NCC decomposition temperature and it is lower than that of the free polymers. The thermal degradation profile of the NCC-grafted polymers is an intermediate of the thermal profile of each

component. This completely shows the grafting of polymers on NCC. Also, char value of the NCC-grafted polymers is higher than the neat polymers as a result of the remained nanocrystals. Degradation temperature of NCC-g-PAA is lower than PAA and also takes place at broad temperature ranges. Random copolymers show two degradation steps in their thermal profiles. Degradation onset is 300 and 317 °C for both of the synthesized copolymers which are higher than the degradation start point of NCC (238 °C) and shows that thermal stability of the NCC increased. The entire polymer grafted NCCs show a two step degradation pattern; the first one relates to the decomposition of NCC and occurs at temperatures in the range of 150-250 °C and the other originates from the copolymers at temperature span of 275-400 °C [38, 62].



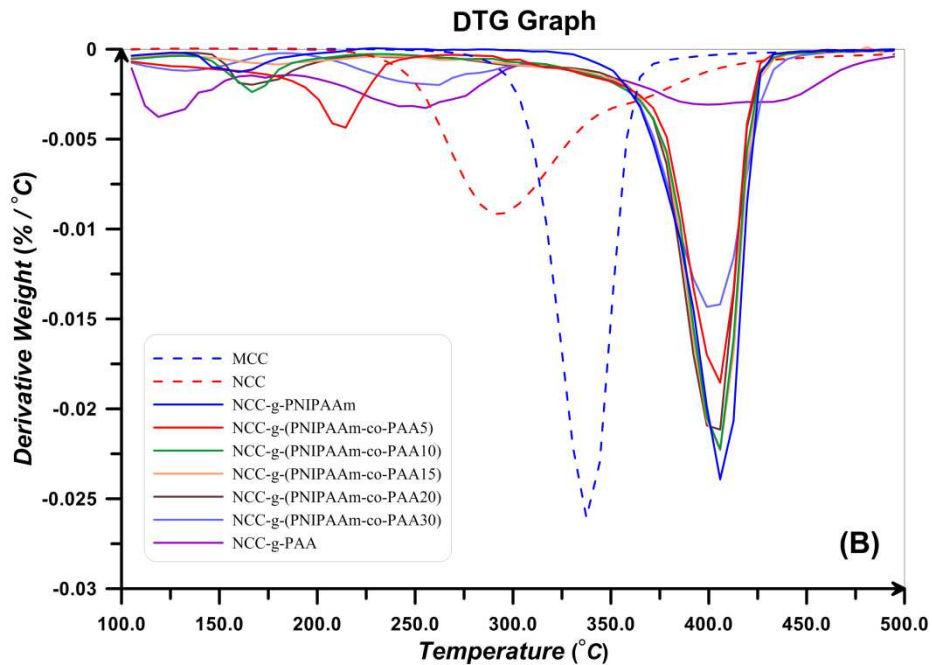


Figure 12- (A) TGA, (B) DTG thermograms for MCC, NCC, and polymer grafted NCCs

Table 4- Degradation start point ($T_{d,s}$, °C), DTG peak point ($T_{d,m}$, °C), and degradation percentage (D, %) for free and NCC-grafted polymers extracted from TGA thermograms

Polymer	1 st Step			2 nd Step			3 rd Step		
	$T_{d,s}$	$T_{d,m}$	D	$T_{d,s}$	$T_{d,m}$	D	$T_{d,s}$	$T_{d,m}$	D
PNIPAAm	285	411	87.4	---	---	---	---	---	---
NCC-g-PNIPAAm	140	160	4.5	340	405	81.3	---	---	---
PNIPAAm-co-pAA5	233	412	90.5	---	---	---	---	---	---
NCC-g-(PNIPAAm-co-pAA5)	115	212	21.8	287	404	67.6	---	---	---
PNIPAAm-co-pAA10	219	248	4.9	284	411	86.6	---	---	---
NCC-g-(PNIPAAm-co-pAA10)	135	167	8.2	300	406	78.4	---	---	---
PNIPAAm-co-pAA15	222	240	4.5	359	410	69.9	---	---	---
NCC-g-(PNIPAAm-co-pAA15)	135	176	5.5	290	406	82.1	---	---	---
PNIPAAm-co-pAA20	210	241	10.3	351	411	72.1	---	---	---
NCC-g-(PNIPAAm-co-pAA20)	145	165	7.9	276	411	80.2	---	---	---
PNIPAAm-co-pAA30	202	241	14.7	343	406	70.8	---	---	---
NCC-g-(PNIPAAm-co-pAA30)	101	134	6.8	191	253	13.9	317	403	68.1
PAA	108	193	19.9	219	269	24.2	312	387	39.2
NCC-gPAA	100	119	15.2	194	252	26.1	318	501	36.1

Relaxation behavior of copolymers by the addition of AA content and also effect of attachment on the chain confinement were evaluated by DSC at the temperature range of 25–250 °C. The curves were obtained after removing thermal history as follows: After a heating procedure, the samples were cooled to room temperature to distinguish the phase conversion and other irreversible thermal behaviors. Subsequently, glass transition as a macroscopic indication of the relaxation behavior was obtained through the second heating cycle. The strength and nature of the interface can result in various T_g values. Graft polymer chains relax in a different manner in comparison with the free chains; this difference indicates interactions between the substrate and chains with covalent bonding [63]. Substrate confinement commonly increases T_g value. DSC results of PNIPAAm, random copolymers, and their nanocomposites are presented in Figure 13. According to the results, glass transition temperature of random copolymers increases by the addition of AA content. Similarly, polymer grafting on NCC results in higher T_g values as a results of confinement of NCC on the relaxation of polymer chains [43]. Heat flow differences near the T_g which can be a rough estimation of heat capacity variation (ΔC_p) are somewhat different in the case of the polymers and its nanocomposites. According to the ΔC_p values derived from DSC results and presented in Table 5, it is concluded that NCC not only confines the segmental motions of the polymers but also it reduces the heat capacity variation at glass transition temperature. Also, by increasing AA content of the copolymers, ΔC_p values decrease. Decrease of molecular weight by the addition of AA content in combination with the increase of a PAA which does not response to the increase of temperature at this temperature region may be the reasons. Decrease of PNIPAAm content in the copolymers by the addition of AA is also concluded by the ratio of ΔC_p values for the free and attached polymers [64].

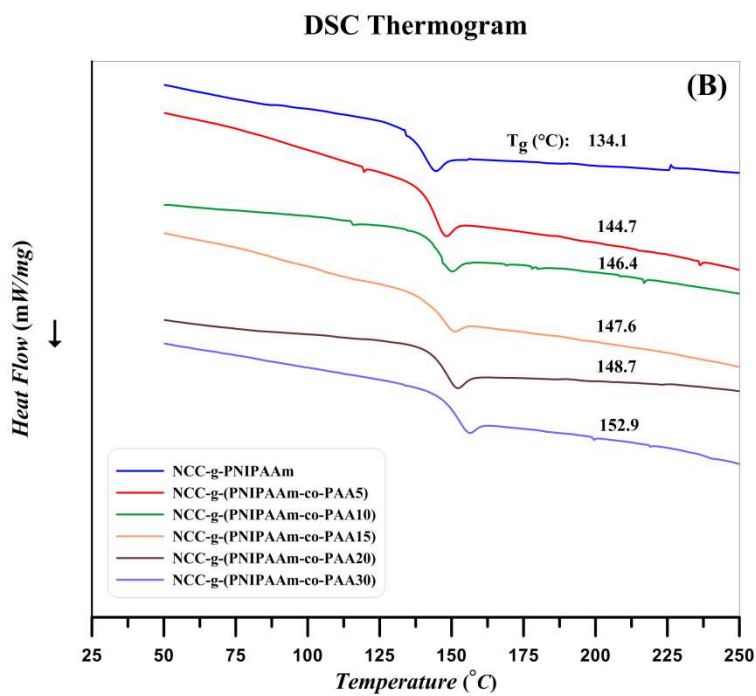
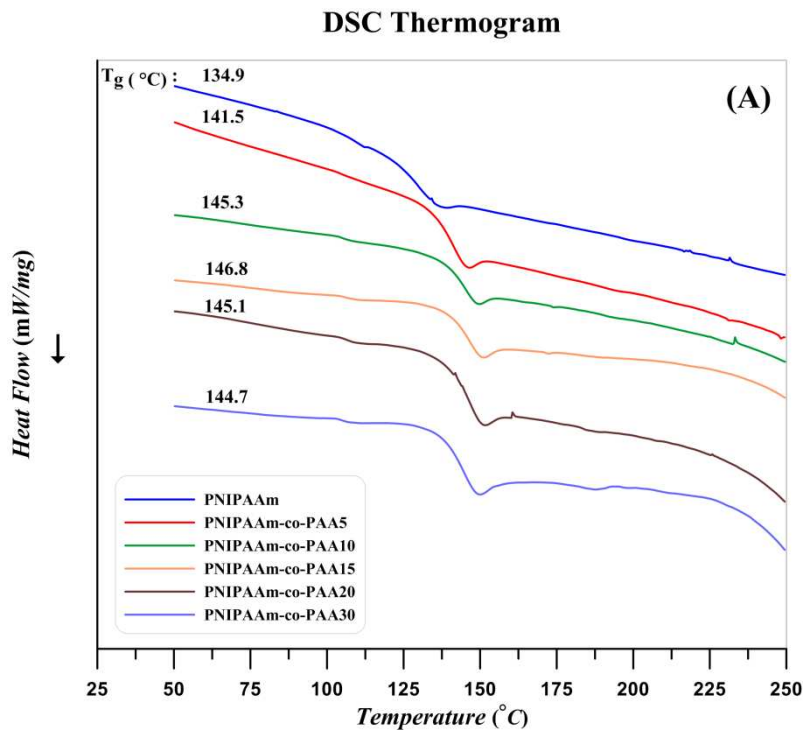


Figure 13- DSC thermograms for (A) free and (B) NCC-grafted PNIPAAm and its random copolymers with AA

Table 5- DSC results of free and NCC attached NIPAAm copolymers

Sample	T _g (°C)		ΔC _p (mW/°C)		%PNIPAAm
	Free	Attached	Free	Attached	
PNIPAAm	134.9	134.1	64.52	55.06	85.3
PNIPAAm-co-pAA5	141.5	144.7	95.64	72.30	75.6
PNIPAAm-co-pAA10	145.3	146.4	87.74	66.49	75.8
PNIPAAm-co-pAA15	146.8	147.6	82.05	61.61	75.0
PNIPAAm-co-pAA20	145.1	148.7	78.72	57.60	73.1
PNIPAAm-co-pAA30	144.7	152.9	79.50	57.49	72.0

XRD results for the MCC, NCC, and also free and NCC-attached polymers are displayed in Figure 14. According to the results, the pattern for MCC and NCC are similar which shows that the crystalline structure of cellulose I was not destroyed upon the hydrolysis with acid. It is clear that the crystalline peak area increases after acid hydrolysis because the amorphous parts of MCC are hydrolysed by the acid. MCC and NCC display four diffraction peaks at 14.8, 16.1, 22.5, and 34.5°, which are typical of cellulose [65, 66]. Two peaks at 14.8 and 16.1° corresponds to the cellulose I polymorph structure and the peak at 22.5° is assigned to the crystalline parts. Degree of crystallinity for MCC and NCC is equals to 69.3 and 68.5% respectively which are in typical crystallinity value range of 55–80% [67]. Decrease of crytallinity degree for NCC is ascribed to its higher amorphous surfaces which is a result of its high aspect ratio [55]. The characteristic peaks of NCC at the diffraction angles of 16.2 and 22.5° are not present in the patterns of NCC-grafted polymers which is a result of its low content in the nanocomposites and also lower diffraction intensity of MCC compared with the polymers. Two peaks at diffraction angles of 8.5 and 20.5° for all the free polymers show their crystalline structure. NCC-grafted polymers, however, show weak peaks at these diffraction angles which is a result of NCC particles [57].

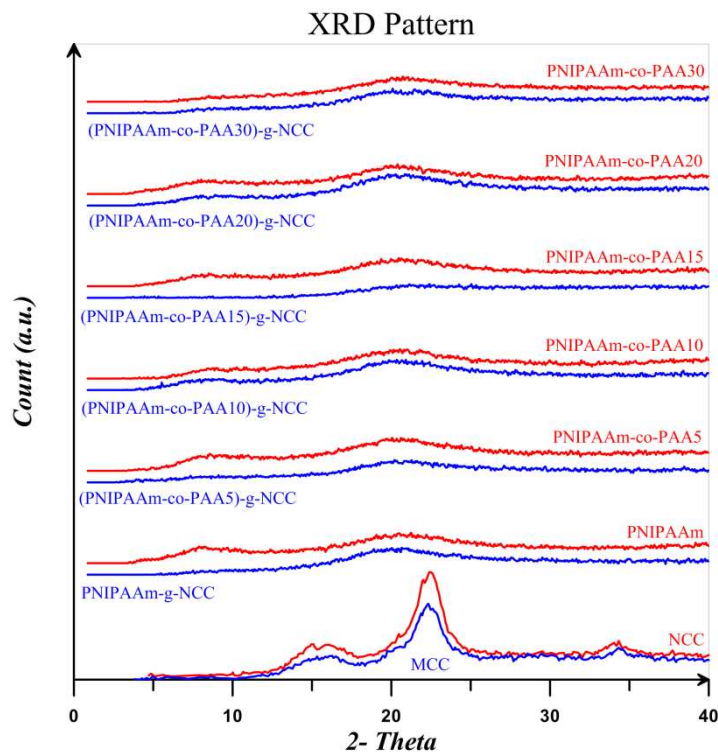


Figure 14- XRD patterns for MCC, NCC, and free and NCC-attached PNIPAAm, PNIPAAm-co-PAA15, and PNIPAAm-co-PAA30

TEM images of the polymer-attached NCC is provided in Figure 15. Because of intra- and intermolecular hydrogen bonding, NCC particles are mainly in the form of clusters as shown in Figure 1 (C). The overall morphology of the nanocrystals has not been changed upon the grafting reaction. However, after polymer grafting, NCC particles observed in the separated forms. Polymer-grafted NCCs show polymer covering of nanocrystals as a layer on them [68].

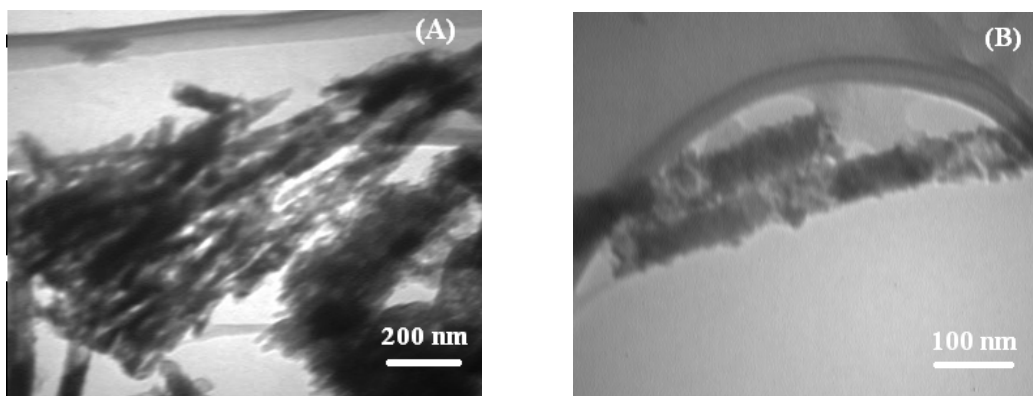


Figure 15- TEM images for polymer attached NCC with two magnifications

4. CONCLUSIONS

Dual-sensitive free and NCC-grafted random copolymers of NIPAAm and AA with different AA contents were synthesized by RAFT polymerization. Grafting reaction was carried out via R-group approach using DDMAT-grafted NCCs. DLS results show that NCC particles with 107 nm in length and narrow size distribution are formed. Rod like shapes of NCC is also displayed in SEM and TEM images. Sulfur content of 6.39% from XPS shows that the graft percent of DDMAT on NCC is about 17.14%. Appearance of the C–S and C=S peaks at the wave numbers of 804 and 1249 cm^{-1} in Raman spectra and also the peak at 1635 cm^{-1} arising from the carbonyl groups of DDMAT are evidences for the successful surface modification of NCC with CTA. ^1H NMR shows that molecular weight of copolymers reduces by the addition of AA content. Addition of NCC, AA content, and pH at higher pH values results in increase of LCST. At low pH values, increase of LCST is occurred by increase of NCC and also pH value. Polymer-grafted NCCs are thermally more stable than NCC. Glass transition temperature of random copolymers increases by the addition of AA content and also NCC. XRD results indicates that by grafting polymers on NCC, their crystalline peaks area diminished. Polymer covering on the NCCs was shown by TEM.

ACKNOWLEDGMENTS

Iran's Research Institute of Petroleum Industry is greatly appreciated for its financial support.

REFERENCES

- 1- X. Yin, A. S. Hoffman, P. S. Stayton, *Biomacromolecules*, 2006, **7**, 1381–1385.
- 2- C. M. Schilli, M. Zhang, E. Rizzardo, S. H. Thang, Y. K. Chong, K. Edwards, G. Karlsson, A. H. E. Müller, *Macromolecules*, 2004, **37**, 7861–7866.
- 3- C. Vasilea, G. G. Bumbua, R. P. Dumitriua, G. Staikos, *Europ. Polym. J.*, 2004, **40**, 1209–1215.
- 4- H. G. Schild, *Prog. Polym. Sci.*, 1992, **17**, 163–249.
- 5- H. Feil, Y. H. Bae, J. Feijen, S. W. Kim, *Macromolecules*, 1993, **26**, 2496–2500.
- 6- G. Chen, A. S. Hoffman, *Nature*, 1995, **373**, 49–52.
- 7- V. Bulmus, Z. Ding, C. J. Long, P. S. Stayton, A. S. Hoffman, *Bioconjugate Chem.*, 2000, **11**, 78–83.
- 8- X. Zhao, W. Liu, D. Chen, X. Lin, W. W. Lu, *Macromol. Chem. Phys.*, 2007, **208**, 1773–1781.
- 9- K. S. Soppimath, D. C. W. Tan, Y. Y. Yang, *Adv. Mater.*, 2005, **17**, 318–323.
- 10- A. F. Olea, J. K. Thomas, *Macromolecules*, 1989, **22**, 1165–1169.
- 11- B. Liu, S. Perrier, *J. Polym. Sci., Part A: Polym. Chem.*, 2005, **43**, 3643–3654.
- 12- P. Bilalis, G. Zorba, M. Pitsikalis, N. Hadjichristidis, *J. Polym. Sci., Part A: Polym. Chem.*, 2006, **44**, 5719–5728.
- 13- K. Nakashima, P. Bahadur, *Adv. Colloid Interface Sci.*, 2006, **123**, 75–96.
- 14- Č. Končák, D. Oupický, V. Chytrý, K. Ulbrich, *Macromolecules*, 2000, **33**, 5318–5320.

- 15- D. Klemm, F. Kramer, S. Moritz, T. Lindström, M. Ankerfors, D. Gray, A. Dorris, *Angew. Chem. Int. Ed.*, 2011, **50**, 2–31.
- 16- P. Lu, Y. L. Hsieh, *Carbohydr. Polym.* 2010, **82**, 329–336.
- 17- Y. Habibi, L. A. Lucia, O. J. Rojas, *Chem. Rev.*, 2010, **110**, 3479–3500.
- 18- R. Rodriguez, C. Alvarez-Lorenzo, A. Concheiro, *J. Controlled Release* 2003, **86**, 253–265.
- 19- C. Ding, X. Qian, J. Shen, X. An, *Bioresearch* 2010, **5**, 303–315.
- 20- K. H. M. Kan, J. Li, K. Wijesekera, E. D. Cranston, *Biomacromolecules* 2013, **14**, 3130–3139.
- 21- K. A. Mahmoud, K. B. Male, S. Hrapovic, J. H. Luong, *ACS Appl. Mater. Interfaces* 2009, **1**, 1383–1386.
- 22- H. Wang, M. Roman, *Biomacromolecules* 2011, **12**, 1585–1593.
- 23- J. V. Edwards, N. Prevost, A. French, M. Concha, A. DeLucca, Q. Wu, *Engineering* 2013, **5**, 20–28.
- 24- E. Lam, K. B. Male, J. H. Chong, A. C. W. Leung, J. H. T. Luong, *Trends Biotechnol.* 2012, **30**, 283–290.
- 25- H. Roghani-Mamaqani, V. Haddadi-Asl, M. Salami-Kalajahi, *Polym. Rev.* 2012, **52**, 142–188.
- 26- W. A. Braunecker, K. Matyjaszewski, *Prog. Polym. Sci.*, 2007, **32**, 93–146.
- 27- H. Roghani-Mamaqani, V. Haddadi-Asl, M. Najafi, M. Salami-Kalajahi, *AIChE J.*, 2011, **57**, 1873–1881.
- 28- H. Roghani-Mamaqani, V. Haddadi-Asl, M. Najafi, M. Salami-Kalajahi, *J. Appl. Polym. Sci.*, 2012, **123**, 409–417.

- 29- S. Rahimi-Razin, M. Salami-Kalajahi, V. Haddadi-Asl, H. Roghani-Mamaqani, *J. Polym. Res.*, 2012, **19**, 9954.
- 30- L. Ahmadian-Alam, V. Haddadi-Asl, H. Roghani-Mamaqani, L. Hatami, M. Salami-Kalajahi, *J. Polym. Res.*, 2012, **19**, 9773.
- 31- S. Rahimi-Razin, V. Haddadi-Asl, M. Salami-Kalajahi, F. Behboodi-Sadabad, H. Roghani-Mamaqani, *J. Iran Chem. Soc.*, 2012, **9**, 777–887.
- 32- O. Glaied, M. Dubé, B. Chabot, C. Daneault, *J. Colloid. Interface Sci.*, 2009, **333**, 145–151.
- 33- G. Morandi, L. Heath, W. Thielemans, *Langmuir*, 2009, **25**, 8280–8286.
- 34- J. Yi, Q. Xu, X. Zhang, H. Zhang, *Cellulose*, 2009, **16**, 989–997.
- 35- J. Yi, Q. Xu, X. Zhang, H. Zhang, *Polymer*, 2008, **49**, 4406–4412.
- 36- M. H. Stenzel, T. P. Davis, A. G. Fane, *J. Mater. Chem.*, 2003, **13**, 2090–2097.
- 37- M. Hernández-Guerrero, T. P. Davis, C. Barner-Kowollik, M. H. Stenzel, *Europ. Polym. J.*, 2005, **41**, 2264–2277.
- 38- D. Roy, J. T. Guthrie, S. Perrier, *Macromolecules*, 2005, **38**, 10363–10372.
- 39- D. Roy, J. S. Knapp, J. T. Guthrie, S. Perrier, *Biomacromolecules*, 2008, **9**, 91–99.
- 40- M. Hiltunen, S. Riihela, S. L. Maunu, *J. Polym. Sci. Part A: Polym. Phys.*, 2009, **47**, 1869–1879.
- 41- R. Fleet, J. B. McLeary, V. Grumel, W. G. Weber, H. Matahwa, R. D. Sanderson, *Europ. Polym. J.*, 2008, **44**, 2899–2911.
- 42- M. Semsarilar, V. Ladmiral, S. Perrier, *J. Polym. Sci.: Part A: Polym. Chem.*, 2010, **48**, 4361–4365.

- 43- M. Barsbay, O. Gu ven, T. P. Davis, C. Barner-Kowollik, L. Barner, *Polymer*, 2009, **50**, 973–982.
- 44- J. T. Lai, D. Filla, R. Shea, *Macromolecules*, 2002, **35**, 6754–6756.
- 45- W. Bai, J. Holbey, K. Li, *Cellulose*, 2009, **16**, 455–465.
- 46- J. Loiseau, N. Doerr, J. M. Suau, J. B. Egraz, M. F. Llaura, C. Ladaviere, *Macromolecules*, 2003, **36**, 3066–3077.
- 47- S. J. Eichhorn, R. J. Young, *Cellulose*, 2001, **8**, 197–207.
- 48- S. Elazzouzi-Hafraoui, Y. Nishiyama, J. L. Putaux, L. Heux, F. Dubreuil, C. Rochas, *Biomacromolecules*, 2008, **9**, 57–65.
- 49- F. Azzam, L. Heux, J. L. Putaux, B. Jean, *Biomacromolecules*, 2010, **11**, 3652–3659.
- 50- S. Elazzouzi-Hafraoui, Y. Nishiyama, J. L. Putaux, L. Heux, F. Dubreuil, C. Rochas, *Biomacromolecules*, 2008, **9**, 57–65.
- 51- Y. Habibi, A. L. Goffin, N. Schiltz, E. Duquesne, Ph. Dubois, A. Dufresne, *J. Mater. Chem.*, 2008, **18**, 5002–5010.
- 52- X. Cao, Y. Habibi, L. A. Lucia, *J. Mater. Chem.*, 2009, **19**, 7137–7145
- 53- Z. Q. Cao, W. G. Liu, G. X. Ye, X. L. Zhao, X. Z. Lin, P. Gao, K. D. Yao, *Macromol. Chem. Phys.*, 2006, **207**, 2329.
- 54- G. Morandi, L. Heath, W. Thielemans, *Langmuir*, 2009, **25**, 8280–8286.
- 55- R. Cha, Z. He, Y. Ni, *Carbohydr. Polym.*, 2012, **88**, 713–718.
- 56- G. Chen, A. Dufresne, J. Huang, P. R. Chang, *Macromol. Mater. Eng.*, 2009, **294**, 59–67.
- 57- M. Salami-kalajahi, V. Haddadi-Asl, F. Behboodi-Sadabad, S. Rahimi-Rezin, H. Roghani-Mamaqani, *J. Polym. Eng.*, 2012, **32**, 13–22.
- 58- C. Y. Hong, C. Y. Pan, *Macromolecules*, 2006, **39**, 3517–3524.

- 59- G. Chen, A. S. Hoffman, *Nature*, 1995, **373**, 49–52.
- 60- I. C. McNeil, S. M. T. Sadeghi, *Polym. Degrad. Stab.*, 1990, **29**, 233–246.
- 61- N. Wang, E. Ding, R. Cheng, *Polymer*, 2007, **48**, 3486–3493.
- 62- H. Roghani-Mamaqani, V. Haddadi-Asl, Kh. Khezri, E. Zeinali, M. Salami-Kalajahi, *J. Polym. Res.*, 2014, **21**, 333.
- 63- M. Yu, R. Yang, L. Huang, X. Cao, F. Yang, D. Liu, *BioResources*, 2012, **7**, 1802–1812.
- 64- J. O. Zoppe, Y. Habibi, O. J. Rojas, R. A. Venditti, L. S. Johansson, K. Efimenko, M. Osterberg, J. Laine, *Biomacromolecules*, 2010, **11**, 2683–2691.
- 65- Y. Nishiyama, P. Langan, H. Chanzy, *J. Am. Chem. Soc.*, 2002, **124**, 9074–9082.
- 66- J. Sugiyama, R. Vuong, H. Chanzy, *Macromolecules*, 1991, **24**, 4168–4175.
- 67- S. Wei, V. Kumar, G. S. Banker, *Int. J. Pharm.*, 1996, **142**, 175–181.
- 68- F. R. Mayo, F. M. Lewis, *J. Am. Chem. Soc.*, 1944, **66**, 1594–1601.

Table of Contents

Nanocrystalline Cellulose Grafted Random Copolymers of N-isopropylacrylamide and Acrylic acid Synthesized by RAFT Polymerization: Effect of Different Acrylic acid Contents on LCST Behavior

Elnaz Zeinali¹, Hossein Roghani-Mamaqani², Vahid Haddadi-Asl¹

¹Department of Polymer Engineering and Color Technology, Amirkabir University of Technology, P.O. Box 15875-4413, Tehran, Iran.

²Department of Polymer Engineering, Sahand University of Technology, P.O. Box 51335-1996, Tabriz, Iran.

Free and nanocrystalline cellulose (NCC)-attached homopolymers of N-isopropylacrylamide and acrylic acid (AA) as temperature- and pH-sensitive materials and also their dual-sensitive copolymers with different contents of AA were synthesized by RAFT polymerization. Addition of NCC, AA content, and pH at higher pH values results in increase of LCST. At low pH values, increase of LCST is occurred by increase of NCC and also pH value. Morphology and crystalline structure of polymer-grafted NCCs were examined by TEM and X-ray diffraction respectively.

